Solid phases of phosphorus carbide: An *ab initio* study

Frederik Claeyssens
Department of Engineering Materials, Sir Robert Hadfield Building, University of Sheffield, Mappin Street, Sheffield S1 3JD, United Kingdom

Judy N. Hart,* Neil L. Allan,* and Josep M. Oliva†
School of Chemistry, University of Bristol, Bristol BS8 1TS, United Kingdom
(Received 12 December 2008; revised manuscript received 10 March 2009; published 23 April 2009)

The thermodynamic stability and properties of different phosphorus carbide phases are studied as a function of composition with first-principles periodic density-functional theory calculations. Calculations are reported for P_4C_3, PC, and P_3C_4 and a range of possible structures examined for each. For P_4C_3, the favored structures are defect zinc-blende structures, while for PC GaSe-like and β-InS-like structures are lowest in energy. For P_3C_4, the lowest-energy structure is a β-C_3N_4-like structure, where phosphorus and carbon occupy sites occupied by carbon and nitrogen, respectively, in the nitride. The importance of the local environments of carbon and phosphorus is emphasized and trends in the preferred environments of C and P are analyzed as a function of composition. For carbon-rich structures, a bonding arrangement with four-coordinate hypervalent phosphorus and sp^2 carbon is preferred, while, for higher phosphorus content, structures containing three-coordinate phosphorus and sp^3 carbon are lower in energy. Comparisons are made with the molecular chemistries of carbon and phosphorus, and also with the corresponding nitrogen analogs. Energies of formation, bulk moduli, and band gaps are calculated for the predicted low-energy phases. The stoichiometry with the lowest formation energy (for $x_P > 0.15$) is PC.

DOI: 10.1103/PhysRevB.79.134115 PACS number(s): 61.50.Ah, 61.66.Fn, 62.20.−x, 71.15.Mb

I. INTRODUCTION

In recent years, considerable efforts have been devoted to carbon nitride, following theoretical predictions that β-C_3N_4 should have a zero-pressure bulk modulus in excess of that of diamond.[1] Unfortunately, preparation of crystalline carbon nitride has proved to be far from straightforward, and to date only small amounts of crystalline material have been synthesized. The nitrogen:carbon ratio in the synthesized materials is often very low[2–5] and the unambiguous identification of crystalline C_3N_4 is difficult due to the small crystal size and the presence of impurities, amorphous material, and a mixture of crystal phases with different compositions.[6,7] One of the most successful methods to make carbon nitride, albeit in the form of nanoparticles, is liquid phase pulsed laser ablation.[8,9] The extreme conditions of high energy, pressure, and temperature achieved with this technique are sufficient to bond together ablated carbon atoms from the target and nitrogen atoms from the liquid to form individual nanosized crystals of C_3N_4. The requirement for such high-energy processes to make C_3N_4 indicates that it is very difficult to incorporate nitrogen into the carbon lattice. Due to these difficulties in producing phase-pure nitrogen-rich carbon nitride with relatively large crystal sizes, it is worthwhile to turn to carbon phosphide analogs. In contrast to the nitrogen situation, phosphorus carbide has been produced as amorphous thin films over a wide range of P:C compositions, up to an atomic ratio of 3:1, by capacitively coupled radio frequency (rf) plasma deposition from gas mixtures of methane and phosphine.[10] However, these films also contain hydrogen from the gas mixture (typically ~10%) and are readily oxidized. Hydrogen-free amorphous films containing carbon and phosphorous can be produced with up to ~28 at. % phosphorus by laser ablation of mixed carbon and phosphorus targets.[11] These experimental developments have led us to start in parallel a theoretical study of phosphorus carbide phases. Our study[11] of the possible structures for PC_3 showed that the lowest-energy structure contained hypervalent phosphorus, four coordinated to carbon. Possible crystal structures of P_4C_3 and PC have been examined recently,[12,13] but structures containing hypervalent phosphorus have not been reported for stoichiometries other than PC_3.

In this work, we study a large number of possible crystalline structures for a range of compositions, with emphasis on those incorporating hypervalent phosphorus. Our focus here is on calculating and rationalizing the lowest-energy structures for P_4C_3, PC, and P_3C_4 by means of periodic *ab initio* density-functional theory (DFT) calculations. Starting structures are selected from analogs from the carbon nitride system [e.g., CN (Refs. 14 and 15) and C_3N_4 (Refs. 1 and 16)] and from those commonly adopted by binary compounds. The results are analyzed together with those previously published for PC_3 (Ref. 11) and P_4C_{3+8n} (n=0–4),[17,18] in order to draw general conclusions regarding the favored environments for carbon and phosphorus.

II. COMPUTATIONAL DETAILS

Calculations in this work were carried out with plane-wave DFT calculations in the generalized gradient approximation (GGA) as implemented in the CASTEP code[19] with the Perdew-Wang exchange correlation functional.[20,21] Only the valence electrons are considered throughout, with the core electrons replaced with ultrasoft Vanderbilt potentials.[22] The energy cutoff for the plane waves was 310 eV. The cell parameters and atomic positions were relaxed and optimized by energy minimization using a conjugate-gradient algorithm

TABLE I. Calculated symmetries, cell parameters, and optimized energies (per formula unit) for different PC structures. Energies are relative to the lowest-energy structure.

Structure	Space group after optimization	Cell parameters	Energy (eV)
β-InS (P–P interlayer bonding)	*Pmnn*	a=2.87 Å, b=4.83 Å, c=6.52 Å	0
GaSe (C–P interlayer bonding)	*P*3*m*1	$a=b$=2.86 Å, c=7.11 Å	0.16
GaSe (C–C interlayer bonding)	*P*3*m*1	$a=b$=2.84 Å, c=7.64 Å	0.19
β-InS (C–P interlayer bonding)	*Pmn*21	a=2.86 Å, b=6.29 Å, c=4.75 Å	0.31
GaSe (P–P interlayer bonding)	*P*3*m*1	$a=b$=2.88 Å, c=7.02 Å	0.35
β-InS (C–C interlayer bonding)	*Pmnn*	a=2.90 Å, b=4.92 Å, c=5.98 Å	1.04
Graphite *ABC*	*P*3*m*1	$a=b$=2.90 Å, c=12.18 Å	0.95
Graphite *AB*	*P*63*mmc*	$a=b$=2.97 Å, c=5.33 Å	0.96
Graphite *AA*	$P\bar{6}m2$	$a=b$=2.96 Å, c=3.50 Å	1.14
bct-4	*I*41*md*	$a=b$=2.92 Å, c=10.47 Å	0.81
H-6	*Pm*	a=2.87 Å, b=2.98 Å, c=7.90 Å α=79.4°	0.87
FeSi	$P2_13$	$a=b=c$=4.80 Å	0.92
MnP	*Pnma*	a=5.40 Å, b=3.63 Å, c=4.48 Å	1.09
ZnO (wurtzite)	*P*63*mc*	$a=b$=2.90 Å, c=5.16 Å	1.18
ZnS (zinc blende)	$P\bar{4}3m$	$a=b=c$=4.20 Å	1.22

with a maximum force tolerance of 0.02 eV $Å^{-1}$ and a maximum stress component of 0.5 GPa. We have checked that the results are well converged with respect to the real-space grid, Brillouin-zone (BZ) sampling, and basis set size. The calculations were repeated with periodic numerical atomic orbital DFT (Refs. 23 and 24) as implemented in the SIESTA code. In this case, the core electrons were replaced with norm-conserving scalar pseudopotentials[25] factorized in the Kleinman-Bylander form.[26,27] A split-valence double-ζ basis set was used, including a set of polarization 3*d* functions on both C and P atoms, as obtained with an energy shift of 250 meV. Periodic hybrid DFT calculations for a selection of the lowest-energy structures for each composition were also carried out with CRYSTAL06,[28] using 6-21G* basis sets for both carbon and phosphorus[29,30] and the B3LYP functional.[31,32] The relative energies of the structures from all three computational approaches are the same, so only results from CASTEP are reported here. Band gaps were calculated by DFT with both GGA (CASTEP) and B3LYP (CRYSTAL06); periodic Hartree-Fock (HF) calculations of the band gap were also performed with CRYSTAL06.

Data for energy as a function of volume were obtained by applying a range of hydrostatic pressures to the structures and carrying out a full geometry optimization of all unit cell parameters and basis atom positions. For layered structures, only positive hydrostatic pressures were applied, while for all other structures both positive and negative pressures were applied.

III. RESULTS

A. PC

For the 1:1 stoichiometry, PC, we have considered a large number of starting structures. Some of these are commonly occurring binary *AB* structures, as listed by Pettifor:[33] GaSe, β-InS (or FeB), NaCl (rocksalt), CsCl, CrB, FeSi, NiAs, CuAu, MnP, cubic ZnS (zinc blende), and hexagonal ZnS (wurtzite). In addition, the structures suggested by Côté and Cohen[15] for CN were examined (i.e., rhombohedral, bct-4, H-6, GeP, and GaSe), as well as layered structures derived from *AA*, *AB*, and *ABC* stackings of phosphorus-substituted graphitic layers. A subset of these structures (rocksalt, zinc blende, rhombohedral, bct-4, H-6, GeP, β-InS, and GaSe) has been studied by Zheng *et al.*,[13] and, in this work, we have further investigated the structures that were reported to be lowest in energy, including a study of the effect of incorporating hypervalent phosphorus.

Overall, the PC structures can be divided roughly into three classes (Table I): (i) the low-lying GaSe- and β-InS-like structures; (ii) two-dimensional (2D) structures without interlayer bonds, which are higher in energy; and (iii) high-energy structures in which atomic valencies are not satisfied (bct-4, FeSi, wurtzite, zinc blende, H-6, CrB, NaCl, NiAs, CsCl, CuAu, and GeP).

For CN, the β-InS and GaSe structures have been found to be the most thermodynamically stable;[15] Côté and Cohen[15] reported that GaSe is the lower in energy of these two structures, while recent new results[34] show the reverse. For PC, the most stable structures of those considered by Zheng *et al.*[13] are also GaSe and β-InS, with GaSe lower in energy than β-InS. By allowing for the possibility of hypervalent phosphorus, we have found additional low-energy structures, which, although related to the GaSe and β-InS structures, have not been considered previously.

There are two possibilities for the individual layers from which both the β-InS-related and GaSe-related structures are constructed. In the first, the phosphorus is three coordinated

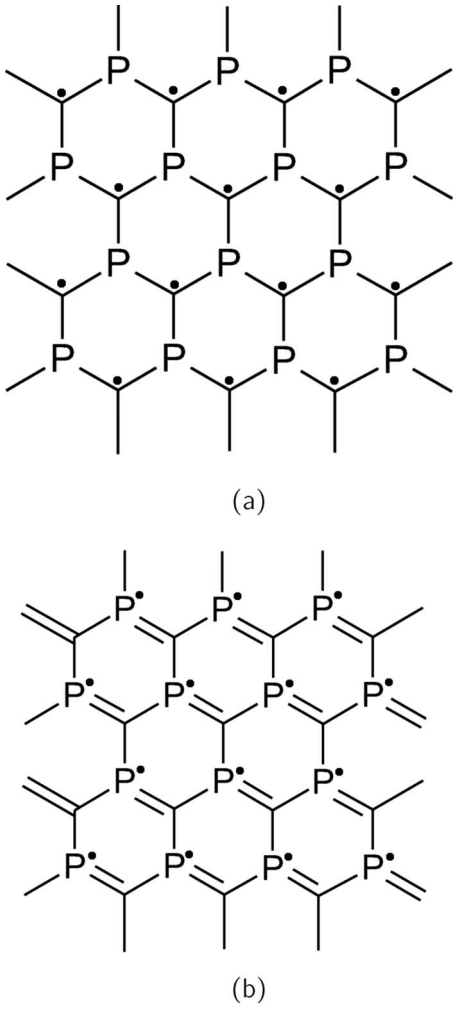

FIG. 1. Structural motifs for the layers from which PC structures are constructed, as described in the text: (a) pattern 1 and (b) pattern 2. Filled circles denote atoms that bond to atoms in an adjacent layer. In structures made from pattern 1 layers, there is one interlayer C–C bond and two P lone pairs per P_2C_2 unit. In structures made from pattern 2 layers, each carbon is three coordinated to P (all in the layer), while each phosphorus is formally hypervalent and four coordinated to three C and one P with an interlayer P–P bond.

to C (all in the same layer), while carbon is four coordinated with three intralayer bonds to P and one interlayer bond [Fig. 1(a)]. Per P_2C_2 unit, there is one C–C bond and two P lone pairs; all bonds are single bonds. We will refer to this bonding pattern as "pattern 1" in the remainder of this paper. In the alternative construction of the layers, "pattern 2" [Fig. 1(b)], each C is three coordinated to P (all in the same layer) while P is four coordinated with three intralayer bonds to C and one interlayer bond, and the bonding within the layers includes C=P double bonds. The pattern 2 layers contain formally hypervalent phosphorus, with the P atoms four coordinated in an approximately tetrahedral arrangement. This is similar to that adopted in several P-containing organic molecules such as $[PhP\text{-}PMe_2{=}C(SiMe_3)_2]_2$.[35]

GaSe-related structures consist of bilayers of these patterns. Bilayers can be constructed from two pattern 1 layers

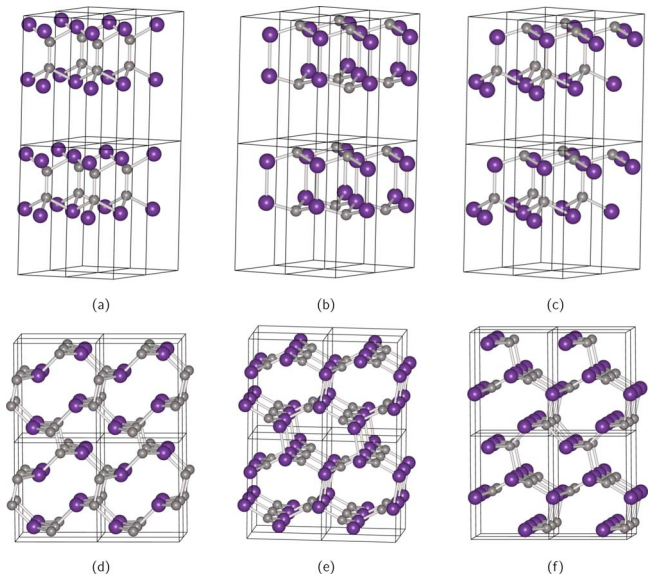

FIG. 2. (Color online) Low-energy PC structures. (a)–(c) GaSe-like structures (*AA* stacking) with C–C, P–P, and C–P interlayer bonding and (d)–(f) β-InS-like structures with C–C, P–P, and C–P interlayer bonding. The structures are made from the motifs shown in Fig. 1 as described in the text. The light gray and the darker purple atoms are C and P, respectively, and the black lines show the unit-cell boundaries. (e) is the lowest-energy structure we have found for PC, while (b) is the highest in energy of these six structures.

(which we denote "bilayer 1" and contains interlayer C–C bonds), two pattern 2 layers ("bilayer 2," containing interlayer P–P bonds), or by combining a pattern 1 layer with a pattern 2 layer ("bilayer 3," containing interlayer C–P bonds) [Figs. 2(a)–2(c)]. We have considered both *AA* and *AB* stackings of the bilayers, giving six possible GaSe-like structures altogether. The GaSe-like structure previously considered[13] for PC corresponds to *AB* stacking of bilayer 1. The results for *AA* stacking of the three bilayers are shown in Table I; there was no significant difference between the energies for *AA* and *AB* stackings, since dispersion interactions are not included in DFT,[36] so the values for *AB* stacking are not included in Table I.

Similarly, various β-InS-like structures can be produced by combining pattern 1 and pattern 2 layers in different combinations. Here, each layer forms interlayer bonds to both of its neighboring layers to give a three-dimensional bonding network. As for GaSe-related structures, there are three possible ways of joining these layers [Figs. 2(d)–2(f)]. In the first, all the individual layers are pattern 1 and there are C–C bonds between layers. In the second, all the individual layers are pattern 2 and there are P–P bonds between layers. In the third, pattern 1 layers alternate with pattern 2 layers and the interlayer bonds are C–P.

The energies of the different possible GaSe-like and β-InS-like structures are similar (Table I), separated by only 0.35 eV/f.u., excluding the β-InS-like with C–C interlayer bonding. For the β-InS-like structures, P–P bonding gives the lowest energy, while in contrast interlayer C–C and C–P bonding gives the lowest energy for the GaSe-like structures.

Within pattern 2 layers, C-P bond lengths are ~1.73 Å, smaller than the bond lengths of ~1.85 Å found in pattern 1 layers, indicating the double-bond character of these layers.[37] From the energy differences between the structures with C–C, C–P, and P–P interlayer bonding for both PC and PC_3 as well as the known bond energies for P–P, C–C, and C–P, we estimate that the hypervalent P–C bonds (with some double-bond character) are ~100–120 kJ mol^{-1} stronger than the P–C single bonds associated with three-coordinate phosphorus.

It is instructive to compare these relative energies with those for similar structures for a stoichiometry richer in carbon, PC_3, which we have examined elsewhere.[11] For bilayer PC_3 structures (analogous to the GaSe-like structures for CP) and also for structures containing three-dimensional bonding networks (analogous to the β-InS-like structures for PC), P–P interlayer bonding gives the lowest energy, while C–C interlayer bonding produces the highest-energy structure. The same behavior is seen for the β-InS-like structures for PC. This suggests that, for both PC and PC_3, structures with four-coordinate phosphorus atoms and three-coordinate carbon atoms are lowest in energy and that the presence of hypervalent phosphorus and, therefore, C=P double-bond character lowers the energy. In such structures, carbon is sp^2 hybridized in a planar geometry and the phosphorus is formally hypervalent and in its preferred tetrahedral geometry. The GaSe-like structure for PC is an exception to this general trend that P–P interlayer bonding gives the lower energy because the three-coordinate carbon is then unable to adopt a planar geometry and is forced into an energetically unfavorable pyramidal arrangement [Fig. 2(b)]. The P-C-P bond angle for the three-coordinate carbon atom is ~113° in the GaSe-like structure, considerably smaller than in the β-InS-like structure (~119°).

Similarly, in the PC_3 bilayer structures,[11] P–P interlayer bonding also forces the three-coordinate carbon atoms out of a perfectly planar geometry, but the average bond angle involving the three-coordinate carbon is at least 116.9°, significantly closer to 120° than in the analogous GaSe-like structure for PC. However, for PC_3, the strain generated because the carbon atoms are unable to attain a perfectly planar geometry means that the energy advantage of replacing C–C interlayer bonds with P–P bonds is less for the bilayer structures than for those containing a three-dimensional network of bonds [0.4 eV/f.u. versus 0.68 eV/f.u.].[11]

For PC, the preference of three-coordinate phosphorus for sp^3 hybridization with a low bond angle can be more easily satisfied in the GaSe-like than in the β-InS-like structure. Consistent with this, for the structures made with only pattern 1 layers, with C–C interlayer layer bonding and three-coordinate phosphorus, the GaSe-like structure has a lower energy (C-P-C bond angle of ~101°) than the β-InS-like (C-P-C bond angle of ~110°–114°).

Again, analogous behavior has been observed for PC_3.[11] For C–C interlayer bonding, the average C-P-C bond angle is lower in the bilayer structure (~100°) than in that containing a three-dimensional bonding network (~107°); the preference of three-coordinate phosphorus for a small bond angle is more easily satisfied in the bilayer structure and the energy is lower than that of the structure with C–C interlayer bonds connecting all the layers in a three-dimensional network.

In the low-energy β-InS-like structure, the P-C-P bond angle is ~119°, which is close to the expected value of 120°, while the P-P interlayer bond length is 2.19 Å, similar to bond lengths of 2.21–2.25 Å in elemental phosphorus.[38] This suggests that the β-InS-like structure is free from distortion and strain. The C–P intralayer bonds are 1.71–1.72 Å and the C-P-C bond angle is ~112°–113°. In contrast, for C–C interlayer bonding in the higher-energy β-InS-like structure, the interlayer bond lengths are ~1.60 Å, longer than the strain-free C-C bond length (1.54 Å), suggesting the presence of significant strain. It is possible that the C–C bond is stretched to increase the nonbonded P-P separation, which is only 2.9 Å; for comparison, the C-C bond length in the GaSe-like structure is 1.54 Å with a nonbonded P-P separation of 3.2 Å. The C–P intralayer bonds in this structure are 1.84–1.87 Å, the average C-P-C bond angle is ~113.5° and the average P-C-P/P-C-C angle is 109.0°.

For the GaSe-like possibilities, P–P interlayer bonding results in a strained structure, with a P-P interlayer bond length of 2.28 Å, and C-P-C and P-C-P bond angles of ~113°, significantly lower than the expected P-C-P bond angle of 120° for three-coordinate carbon. C–C interlayer bonding gives a relatively strain-free structure and is lower in energy, with a C-C bond length of 1.54 Å, C-P-C bond angles of ~101° and an average P-C-P/P-C-C bond angle of 109.0°.

When the symmetry is constrained, the graphitic PC structures are higher in energy than the GaSe-like and β-InS-like structures (Table I). When the symmetry constraint is removed, the graphitelike sheets buckle and interlayer P–P bonds form, such that optimization yields low-energy GaSe-like structures. This is consistent with the preference of phosphorus to adopt a pyramidal rather than planar geometry; phosphorus is able to adopt a hypervalent configuration in order to attain this pyramidal geometry.

Finally, the highest-energy structures for PC are those in which the atomic valencies are not satisfied. Of these structures, the ones in which all atoms have trigonal planar coordination (bct-4, FeSi, H-6) are lowest in energy, followed by those with tetrahedral coordination (MnP, wurtzite, zinc blende). Structures with higher atomic coordination are higher in energy (>−335.0 eV/f.u.).

Previous results[11,13,15] have suggested that the lowest-energy structures of PC and CN are the same, in sharp contrast to C_3P_4/C_3N_4, for which the most stable nitride structures are relatively high in energy for the phosphorus system and vice versa.[17] However, our results for PC here (in addition to recent new results for CN)[34] show that this is not so and, as for C_3P_4/C_3N_4, the structures that are lowest in energy for CN are relatively high in energy for PC. As for C_3N_4,[1] graphitic forms of CN are lowest in energy,[34] but these are high in energy for PC. This preference for diamondlike structures, rather than graphitic structures, is in accordance with the known molecular chemistries of nitrogen and phosphorus.[38] These known differences in the chemistries of nitrogen and phosphorus are also consistent with the relative energies of the diamondlike structures. The lowest-energy structure for PC is the same as the lowest-energy diamondlike CN structure, but with the positions of

the carbon and group 15 element swapped. In Secs. III B and III C, we will show that the same is the case for C_3N_4/P_3C_4 structures. Previously published work,[11] together with new results for carbon nitride,[34] indicates that this is also true for C_3N/PC_3. In the nitride structures, nitrogen is limited to being three coordinated, which means that carbon must occupy the four-coordinate sites. Swapping the positions of the carbon and group 15 element gives structures that are low in energy for phosphorus carbides because it satisfies the preferences of phosphorus for a pyramidal geometry and carbon for sp^2 hybridization.

Antisite defects in PC were briefly studied, swapping one carbon and phosphorus per C_8P_8 unit in the low-energy β-InS-like and GaSe-like structures with P–P and C–C interlayer bonding, respectively. This yielded relatively low-energy structures, with an energy of only 0.26 eV/f.u. (for β-InS) and 0.20 eV/f.u. (for GaSe) higher in energy than the corresponding lowest-energy PC structures. The bonds in the resulting structures are strained due to the change in the bonding arrangement. However, it is not surprising that the structures with antisite defects are only slightly higher in energy than the defect-free structures, since the separation of all of the InS-like and GaSe-like structures with different interlayer bonding is only 0.35 eV/f.u. (excluding the high-energy β-InS-like structure with C–C interlayer bonding).

Overall, we conclude that there is a group of related structures with similar low energies for PC and, therefore, synthesis of phosphorus carbide is likely to result in production of several different structures. Structures containing sp^2 phosphorus are very unstable. The lowest energy is obtained with sp^2 carbon and tetrahedral hypervalent phosphorus, provided that the structure is relatively strain-free. For PC, structures with three-coordinate phosphorus and sp^3 carbon are only marginally higher in energy than those with hypervalent phosphorus and sp^2 carbon. In the GaSe-related and β-InS-like structures, when hypervalent four-coordinate phosphorus is replaced with three-coordinate phosphorus, some C–P double bonds are introduced into the intralayer bonds, resulting in a decrease in energy, but this is always accompanied by a change from C–C interlayer bonding to weaker P–P bonding, which causes the energy to increase. For a P:C ratio of 1, there is an approximate energy balance between these two bonding arrangements. Structures that include hypervalent phosphorus have not been previously investigated for PC, so previous results[13] have indicated that stable phosphorus carbide structures tend to contain three-coordinated phosphorus and four-coordinated carbon. As shown in Secs. III B and III C, this is only so when the P:C ratio is greater than 1.

The energy versus volume curves for the low-energy PC structures and corresponding bulk moduli calculated by fitting to the Birch-Murnaghan equation of state[39] are shown in Fig. 3 and Table II, respectively. For the 2D networks (GaSe-like structures), the bonding between the layers is governed by dispersion interactions, which are not accounted for in DFT. Under a negative hydrostatic stress, the interlayer separation increases, but otherwise the structure remains essentially unchanged. This is consistent with the observation that, under a negative pressure, the energy-volume relationship is almost flat (Fig. 3). For the β-InS-like structures, the structure broke down to form the corresponding GaSe-like structures under negative hydrostatic pressures between −15 and −20 GPa. The β-InS-like structures have higher bulk moduli (~160–220 GPa) than the GaSe-like structures (<10 GPa), as expected due to the weak interlayer bonding in the GaSe-like structures. Structures with C–C interlayer bonding have higher bulk moduli than those with P–P interlayer bonding, while C–P interlayer bonding gives an intermediate bulk modulus, consistent with the change in the strength of the bonding (e.g., the introduction of relatively strong C–C bonds). The bulk moduli of the β-InS-like structures are lower than the bulk modulus of diamond (443 GPa) (Ref. 40) and that calculated for β-C_3N_4 and pseudocubic C_3N_4 (451 and 448 GPa, respectively).[1] However, they are similar to the bulk modulus of MgO or Fe (160 and 168 GPa, respectively)[40,41] and it is also worth bearing in mind typical bulk moduli for the so-called "hard" materials, such as Al_2O_3 (252 GPa), SiC (225 GPa), and β-Si_3N_4 (259 GPa).[40]

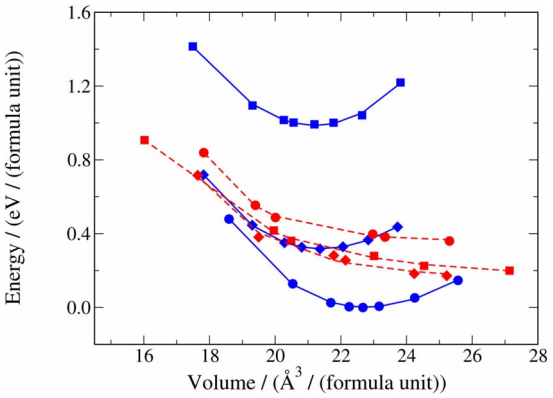

FIG. 3. (Color online) Energy as a function of volume for the low-energy CP structures shown in Fig. 2 (blue solid line: β-InS-like structures; red dashed line: GaSe-like structures; squares: C–C interlayer bonding; circles: P–P interlayer bonding; diamonds: C–P interlayer bonding). The lines show the fits of the data to the Birch-Murnaghan equation of state. Energies are relative to the lowest-energy structure.

Investigation of the band structure of the low-energy PC structures (with DFT and GGA) indicates that they have finite band gaps (consistent with periodic Hartree-Fock and

TABLE II. Equilibrium bulk modulus B_0, volume V_0, and energy E_0, for the low-energy PC structures, calculated from the energy versus volume curves by a fit to the Birch-Murnaghan equation of state (Ref. 39). Energies are relative to the lowest-energy structure.

Structure	K_0 (GPa)	V_0 (Å^3/f.u.)	E_0 (eV/f.u.)
GaSe (C–C interlayer bonding)	7.5	30.7	0.18
GaSe (P–P interlayer bonding)	1.5	29.2	0.36
GaSe (C–P interlayer bonding)	1.7	32.6	0.16
β-InS (C–C interlayer bonding)	222	21.2	0.98
β-InS (P–P interlayer bonding)	157	22.8	0
β-InS (C–P interlayer bonding)	172	21.4	0.31

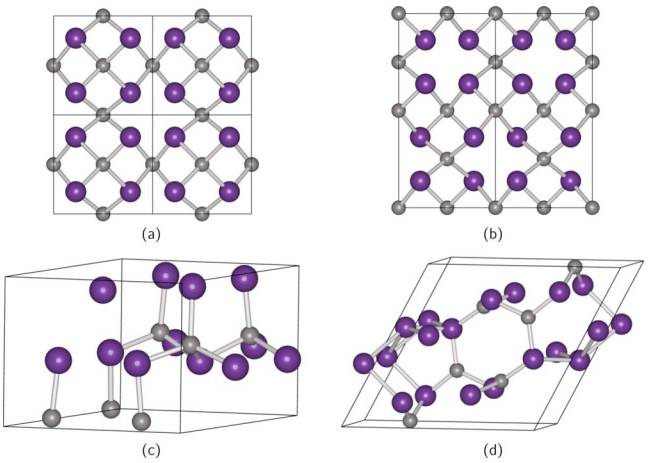

FIG. 4. (Color online) Calculated low-energy structures for crystalline P_4C_3: (a) the pseudocubic structure with a primitive cell containing 1 f.u., (b) the tetragonal structure based on doubling the pseudocubic unit cell, as described in the text, (c) hexagonal defect wurtzite structure, and (d) structure derived from β-C_3N_4, but with the positions of the carbon and group 15 element swapped with respect to the nitride structure, as described in the text. The light gray and the darker purple atoms are C and P, respectively, and the black lines show the unit-cell boundaries.

B3LYP calculations in CRYSTAL06).[28] The GaSe-like bilayer 1 structure exhibits a direct band gap of 1.51 eV (with GGA), which is in excellent agreement with the previously calculated value of 1.6 eV.[13] The other structures exhibit indirect band gaps. For the β-InS-like structures, C–C interlayer bonding gives a smaller band gap than P–P interlayer bonding. The reverse is true for the GaSe-related structures, with C–C interlayer bonding giving a larger band gap than P–P interlayer bonding; it is likely that this is related to the highly strained nature of the structure with P–P interlayer bonding.

The Mulliken charges on the four-coordinate phosphorus atoms (pattern 2) are significantly more positive than the three-coordinate phosphorus (pattern 1) (1.1e versus 0.7e). For the structures made from alternating pattern 1 and pattern 2 layers, there is a charge transfer from the pattern 1 layer to the pattern 2 layer of 0.4e per C_2P_2 unit, indicating that the layer with hypervalent phosphorus carries a net negative charge and, therefore, there is a dipole perpendicular to the layers along the c axis.

B. P_4C_3

It has been previously reported[17,18] that for P_4C_3 the pseudocubic structure [Fig. 4(a)], based on a defect zinc-blende structure, is lowest in energy. However, based on the results for PC presented here, we suspected that there may be other, closely related structures, as well as structures containing hypervalent phosphorus, that are similarly low in energy, so a more detailed search for low-energy structures was conducted.

We begin by investigating the effect of different vacancy orderings for the possible P_4C_3 structures considered in our previous study.[17] The unit cell of the pseudocubic structure investigated previously (space group $P\bar{4}3m$) contains only 1 P_4C_3 f.u. For larger unit cells containing more than 1 f.u., a different vacancy ordering is possible,[42] obtained by doubling the unit cell along one cubic axis (which we specify as the c axis) and displacing the vacancies in alternate planes along this axis by $\frac{1}{2}(\mathbf{a}+\mathbf{b})$ with respect to each other. This gives a body-centered tetragonal structure [space group $I\bar{4}2m$, Fig. 4(b)], analogous to that of $CdAl_2S_4$.

The difference between the energies of this tetragonal structure and the pseudocubic structure is negligible and they are the most stable of all the P_4C_3 structures that we have considered (Table III). Both have P_3C_3 six-membered rings in chair conformations. The pseudocubic and tetragonal structures have C-P bond lengths of 1.86 Å and 1.85–1.87 Å, respectively, with C-P-C bond angles of 103.7° in the pseudocubic structure and 103.3° and 103.7° in the tetragonal structure. The average P-C-P bond angle in both structures is ~109.6°. These bond angles and bond lengths are close to the known values for carbon and phosphorus in strain-free environments (C-P single bond length of 1.85 Å, C-P-C bond angle of ~99°, and an sp^3 carbon bond angle of 109.5°).[43]

As for the defect zinc-blende structure, there are many possible vacancy orderings for the defect wurtzite structure. Doubling the primitive unit cell of the undefective wurtzite structure (P_2C_2) in the a direction and removing one carbon atom from the resulting P_4C_4 unit cell produces a monoclinic structure. Further structures can be obtained, by doubling both the a and b directions of the unit cell of the undefective wurtzite structure and removing two carbon atoms, producing either an orthorhombic or hexagonal structure.

The optimized hexagonal structure ($P63mc$) contains three-coordinate phosphorus and four-coordinate carbon [Fig. 4(c)], as for the defect zinc-blende structures, and has a similarly low energy (Table III). The calculated bond lengths and bond angles are similar to those in the defect zinc-blende structures, although there are small distortions of the bond angles, which may account for the slightly higher energy relative to zinc blende. With the alternative vacancy orderings, the carbon vacancies are closer together and there are some phosphorus atoms adjacent to both vacancies; the optimized structures are highly distorted and contain P–P bonds and these are high in energy (Table III).

Various graphitic structures of P_4C_3 have also been investigated, including both AB and ABC stackings of the graphite sheets proposed by Teter and Hemley[1] [hexagonal unit cell, Fig. 5(a)] and AA and AB stackings of the different vacancy orderings suggested by Alves *et al.*[44] [orthorhombic unit cell, Fig. 5(b)]. However, these graphitic structures have been found to be relatively high in energy (higher than both the defect zinc-blende and defect wurtzite structures, Table III). In all cases, if the symmetry is constrained, intralayer P–P bonds formed [Fig. 6(a)], although these are relatively long (2.4–2.5 Å, compared with ~2.2 Å in elemental phosphorus), indicating that these bonds are weak. When all symmetry constraints were removed, the graphitelike sheets distorted, interlayer bonds formed, and the phosphorus atoms adopted a pyramidal geometry [Fig. 6(b)]. The energy decrease associated with this change is ~0.3 eV/f.u. for the

TABLE III. Calculated symmetries, cell parameters and optimized energies (per f.u.) for different P_4C_3 structures. Energies are relative to the lowest-energy structure.

Structure		Space group after optimization	Cell parameters	Energy (eV)
Defect Zinc blende	Pseudocubic	$P\bar{4}3m$	$a=b=c=4.13$ Å	0
	Tetragonal	$I\bar{4}2m$	$a=b=4.12$ Å, $c=8.31$ Å	0.06
Structures low in energy for C_3N_4[a]	β[b]	$P21m$	$a=7.79$ Å, $b=8.33$ Å, $c=3.01$ Å, $\gamma=119.5°$	0.23
	Cubic	$P1$	$a=6.40$ Å, $b=5.80$ Å, $c=4.85$ Å, $\alpha=97.7°$, $\beta=115.8°$, $\gamma=118.0°$	0.29
Defect wurtzite	Hexagonal	$P63mc$	$a=b=5.80$ Å, $c=4.87$ Å	0.35
	Orthorhombic	$P12$	$a=6.40$ Å, $b=5.80$ Å, $c=4.85$ Å, $\gamma=122.3°$	0.56
	Monoclinic	Pm	$a=4.86$ Å, $b=2.95$ Å, $c=5.01$ Å, $\beta=91.8°$	1.20
Graphitic[c]	Orthorhombic, AB	$Cmm2$	$a=6.50$ Å, $b=5.83$ Å, $c=5.10$ Å	1.12
	Hexagonal, ABC	$R3m$	$a=b=5.75$ Å, $c=11.23$ Å	1.26
	Hexagonal, AB	$Amm2$	$a=7.52$ Å, $b=5.76$ Å, $c=9.98$ Å	1.29
	Orthorhombic, AA	$Pmm2$	$a=3.61$ Å, $b=5.70$ Å, $c=5.02$ Å	1.43
Structures low in energy for C_3N_4 [c]	α	$P31c$	$a=b=8.21$ Å, $c=5.77$ Å	1.39
	β	$P\bar{3}$	$a=b=7.70$ Å, $c=3.07$ Å	1.88
	Cubic	$I\bar{4}3d$	$a=b=c=6.90$ Å	3.20

[a]Structure refers to the initial geometry prior to optimization; geometry optimization was carried out without symmetry constraints and resulted in significant changes in geometry and symmetry.
[b]Positions of carbon and group 15 element interchanged relative to the C_3N_4 structure (as discussed in text).
[c]Optimized with symmetry constraints applied.

structures based on the orthorhombic unit cell and ~1.2 eV/f.u. for those based on the hexagonal unit cell. The structure based on *ABC* stacking of the hexagonal unit cell transformed to a low symmetry form of the pseudocubic structure. This behavior indicates, as for PC, that structures with sp^2 hybridized phosphorus atoms are unstable.

The α-, β-, and cubic-C_3N_4 structures, which are low in energy for carbon nitride, are high in energy for P_4C_3, when they are optimized with symmetry constraints (Table III). In carbon nitride, the carbon is four coordinated and nitrogen is three coordinated with a high C-N-C bond angle ($\geq$115°). Phosphorus, in contrast, prefers a low C-P-C bond angle, which is difficult to achieve in these structures without causing significant strain and distortion, hence resulting in the high energy of these structures for C_3P_4. When the symmetry constraints are released, rearrangement of the structures occurs and P–P bonds form, such that all of the phosphorus adopts a pyramidal geometry and some is four coordinated and hypervalent. The energies in this case are significantly lower; for the α and β phases, the optimized structures are highly disordered, but for the cubic structure the optimized structure is relatively strain-free and the energy is lower than that of the hexagonal defect wurtzite structure, which contains three-coordinate phosphorus and four-coordinate carbon (Table III). Similarly low energies can be achieved by swapping the carbon and phosphorus positions in the initial C_3N_4 structures, such that phosphorus is four coordinated and carbon is three coordinated, and then substituting some carbon for phosphorus to restore the correct stoichiometry. This again results in structures containing four-coordinate hypervalent phosphorus, with some P–P bonds; for the β phase, the optimized structure is almost as low in energy as the defect zinc-blende structures [Fig. 4(d) and Table III]. The low energy of phosphorus carbide structures produced by swapping the positions of carbon and the group 15 element relative to carbon nitride structures has already been noted for PC and this idea will be revisited for P_3C_4 in Sec. III C.

Overall, the lowest-energy P_4C_3 structures are those that contain phosphorus in a pyramidal geometry, as for PC and PC_3. However, in the relatively carbon-rich materials (e.g., PC and PC_3), the lowest-energy structures contain four-coordinate hypervalent phosphorus and sp^2 carbon. More phosphorus-rich P_4C_3 structures with three-coordinate carbon and four-coordinate phosphorus must also contain a significant number of P–P bonds, which are energetically less favorable than P–C bonds; although the low-energy structure for PC contains some P–P bonds, the ratio of P–P to C–P bonds is only 1:6, whereas it would have to be greater than 1:3 for all the phosphorus to be four coordinated in P_4C_3. Thus, for P_4C_3, the lowest energy is attained for structures with three-coordinate phosphorus (and a low C-P-C bond angle) and four-coordinate carbon, with only C–P bonding. The pseudocubic structure meets these criteria and also allows a low C-P-C bond angle and strain-free C–P bonds, thus giving the lowest energy of all structures investigated for

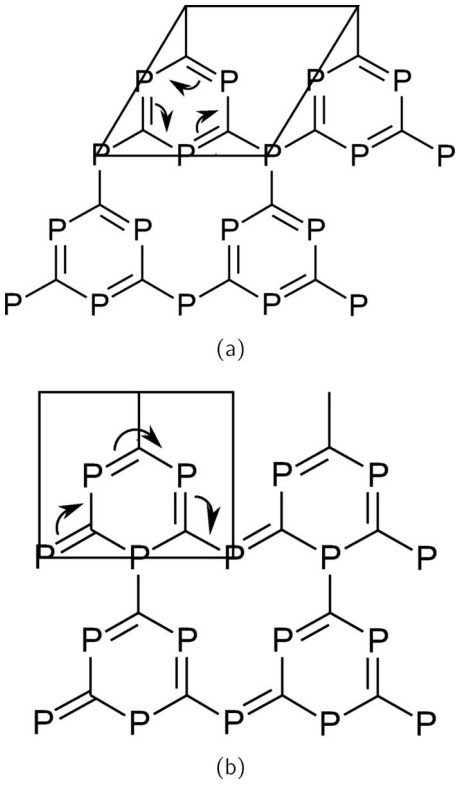

FIG. 5. Possible vacancy orderings for the P_4C_3 graphitic structures considered in this study: (a) hexagonal unit cell following Teter and Hemley (Ref. 1) and (b) orthorhombic unit cell following Alves *et al.* (Ref. 44). Electrons are delocalized only within the P_3C_3 rings in the hexagonal structure, whereas they are delocalized across the graphitelike sheets in the orthorhombic structure.

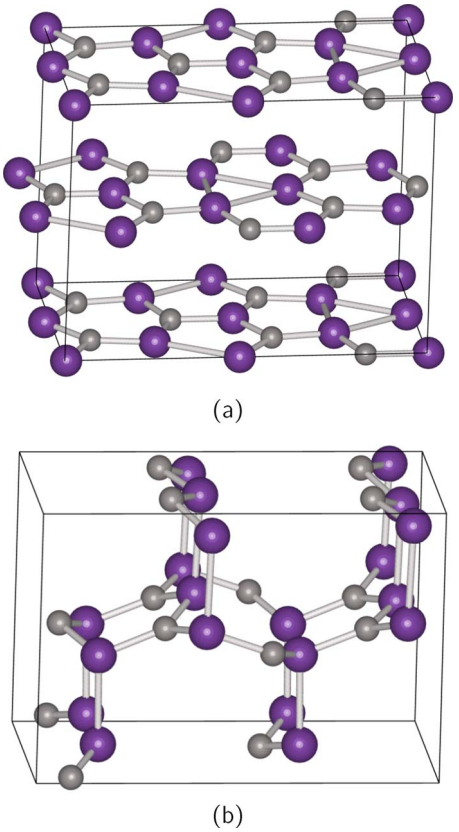

FIG. 6. (Color online) An example of the rearrangement of bonds that occurs for graphitic P_4C_3 structures: bonding pattern after optimization of the P_4C_3 structure based on *AB* stacking of the hexagonal graphite sheets proposed by Alves *et al.* (Ref. 44): (a) symmetry constrained during geometry optimization and (b) no constraints applied during geometry optimization. The light gray and the darker purple atoms are C and P, respectively, and the black lines show the unit-cell boundaries.

P_4C_3. However, changing the vacancy ordering in the pseudocubic structure does not significantly change the energy. Consistent with results for PC, this suggests that the products of attempts to synthesize these materials are likely to contain a mixture of different structures, predominantly based on defect zinc blende, but with disordered vacancies and low symmetry. In addition, even for this relatively phosphorus-rich stoichiometry, there are some structures containing hypervalent phosphorus that are only marginally higher in energy than the lowest-energy structures containing only three-coordinate phosphorus.

As for PC versus CN, these results show that structures low in energy for C_3N_4 are high in energy for P_4C_3. For example, graphitic forms for P_4C_3 are higher in energy than diamondlike forms, while for C_3N_4 the graphitic structures are lowest in energy.[1] Of the diamondlike structures, the lowest-energy nitride structures are the α and β phases, with four-coordinate carbon and three-coordinate nitrogen in a planar geometry. In contrast, the lowest-energy structure for P_4C_3, the pseudocubic structure, in which the three-coordinate phosphorus is able to adopt a pyramidal geometry with a low C-P-C bond angle, is high in energy for C_3N_4. These differences in the relative energies of the nitrogen and phosphorus-containing structures are consistent with the much stronger preference of phosphorus, compared with nitrogen, for sp^3 hybridization.[38]

Antisite defects have been investigated by exchanging a carbon and phosphorus within a $2\times2\times2$ supercell of the lowest-energy pseudocubic ($P\bar{4}3m$) structure, followed by reoptimization. The resulting optimized structure is only 0.17 eV higher in energy than the starting pseudocubic structure. This antisite-pair formation energy is much lower than for silicon carbide (3.5 eV).[45] The low energy of defect formation indicates that, just as there are various P_4C_3 structures with different vacancies orderings with similar energies, there may also be a range of disordered structures with similar energies for P_4C_3. In the defect-free pseudocubic structure, the C-P-C bond angles for the three-coordinate phosphorus are low. When an antisite defect is introduced, the carbon atom in the three-coordinated site is in a highly strained geometry, because it is difficult for it to be planar in this structure. This suggests that it is unfavorable to have carbon in the three-coordinate sites in the pseudocubic structure. This has implications for using this structure as a candidate for P_3C_4 by interchanging carbon and phosphorus, a point to which we return when we discuss P_3C_4 (Sec. III C).

The calculated bulk modulus of the pseudocubic phase of P_4C_3, obtained by a fit of the calculated energy versus vol-

TABLE IV. Calculated symmetries, cell parameters, and optimized energies (per f.u.) for different P_6C_8 structures. Energies are relative to the lowest-energy structure.

Structure	Space group after optimization	Cell parameters	Energy (eV)
β-InS-like	Pm	a=2.80 Å, b=33.6 Å, c=6.63 Å	0
β-C_3N_4-like[a]	$P\bar{3}$	$a=b$=7.69 Å, c=5.64 Å	0.10
α-C_3N_4-like[a]	$P3$	$a=b$=7.81 Å, c=5.53 Å	0.75
Cubic-C_3N_4-like[a]	$P1$	a=6.42 Å, b=6.46 Å, c=6.45 Å α=92.2°	1.17
β-C_3N_4 [b]	$R\bar{3}$	$a=b$=7.78 Å, c=8.71 Å	0.55
α-C_3N_4 [b]	$P31c$	$a=b$=8.21 Å, c=5.77 Å	0.89
Cubic-C_3N_4 [b]	$I\bar{4}3d$	$a=b=c$=6.73 Å	1.54
Defect wurtzite, monoclinic	Pm	a=4.86 Å, b=5.69 Å, c=7.19 Å β=106.4°	1.70
Defect wurtzite, orthorhombic	$P21$	a=5.68 Å, b=5.11 Å, c=5.61 Å β=95.0°	3.05
Defect zinc blende, tetragonal	$I\bar{4}2m$	$a=b$=4.11 Å, c=8.37 Å	3.48
Defect wurtzite, hexagonal	$P63mc$	$a=b$=5.82 Å, c=4.79 Å	4.15
Defect zinc blende, pseudocubic	$P\bar{4}3m$	$a=b=c$=4.09 Å	5.04
Graphitic, hexagonal AB	$Amm2$	a=8.70 Å, b=5.70 Å, c=10.02 Å	11.12

[a]Structure contains one C–C bond per P_6C_8 f.u.
[b]Structure without C–C bonds.

ume curve to the Birch-Murnaghan equation of state,[39] is 158 GPa. This is somewhat lower than the estimate of Ding and Feng[46] (209 GPa), but as for PC it is similar to the typical bulk moduli for the so-called hard materials.

DFT predicts P_4C_3, in the low-energy pseudocubic structure, to be metallic, in agreement with previous results.[12,46] This observation has been further studied by a periodic HF calculation, and also a DFT calculation with the B3LYP hybrid functional, for the optimized pseudocubic C_3P_4 structure with CRYSTAL06.[28] Calculations at both levels give band diagrams that are similar in shape, but HF predicts a direct band gap of 3.9 eV at the Γ point, while B3LYP indicates metallic behavior. It is well known[47] that local-density approximation (LDA) and GGA calculations underestimate the band gap, while it is usually overestimated in HF theory. Thus we are unable at this stage to draw firm conclusions about the band gap of C_3P_4. However, the small, or nonexistent, band gap for this material, where all phosphorus is three coordinated, is consistent with those for the β-InS-related structures for PC, where the structure with three-coordinate phosphorus has a smaller band gap than the structure with three-coordinate carbon.

We have also studied the electron distribution in C–P bonds in pseudocubic P_4C_3 and compared it with that in C–N bonds of the C_3N_4 analog. The density along C–P(N) internuclear axis shows a distinct polarization of the density toward C in the C–P bond, but N in the C–N bond. This is in accordance with the relative electronegativities of C, P, and N, and also with the Mulliken population results for the pseudocubic phase, with values of $-0.90e$ for C and $+0.67e$ for P. For the graphitic phase, the bond is slightly more polar ($-0.99e$ for C and $+0.74e$ for P on average), as would be expected for the more electronegative sp^2 hybridized carbon. These values are similar to those noted for PC.

C. P_3C_4

For both PC (as discussed above) and PC_3,[11] the lowest-energy structures include some C–P double bonding, and the phosphorus atoms are four coordinated and hypervalent, while the carbon atoms have sp^2 character. The opposite is true for the low-energy P_4C_3 structures, with phosphorus three coordinated and carbon four coordinated. Therefore, we have formed possible structures for the P_3C_4 stoichiometry by interchanging the positions of the P and C atoms in the P_4C_3 structures.

In contrast to P_4C_3, the β-C_3N_4, α-C_3N_4, and cubic-C_3N_4 structures are all lower in energy than the pseudocubic (defect zinc-blende) and defect wurtzite structures for P_3C_4 (Table IV). The energy ordering within the groups of the defect zinc-blende and defect wurtzite structures is the opposite of that for P_4C_3. For both P_4C_3 and P_3C_4, the graphitic structures are high in energy.

These results indicate that, overall, the energy ordering of the diamondlike structures for P_3C_4 is the reverse of the energy ordering found in the P_4C_3 structures. In the P_4C_3 structures, the three-coordinate atom (phosphorus) prefers a pyramidal geometry, whereas in the P_3C_4 structures the three-coordinate atom is carbon, which prefers a planar geometry.

In these P_3C_4 structures, the carbon atoms are sp^2 hybridized while the phosphorus atoms exhibit hypervalent bonding and all bonds are P–C bonds with no C–C or P–P bonds. Thus, we expect to form a network in which the bonds have some double-bond character, and in which the sp^2 carbon

atoms have P-C-P angles of 120° and the phosphorus atoms are tetrahedral with C-P-C bond angles of ~109°. Any distortion of this "ideal" network will result in a higher-energy structure. Indeed, in the lowest-energy β-C_3N_4 structure, the C-P bond lengths are 1.73–1.74 Å, while the average P-C-P bond angle is 120°, with C-P-C angles in the range of 107.0°–112.0° (average 109.5°). These values suggest that this is a strain-free bonding network for P_3C_4. Higher-energy structures show considerable strain, particularly around the sp^2 carbon atoms. In the α-C_3N_4 structure, the carbon sites have average P-C-P bond angles as low as 117.5°. Thus, the relatively high energy of the α-C_3N_4 may be related to the low P-C-P bond angles, while the high energy of the cubic structure may be associated with the higher density of this phase and, thus, the shorter nonbonded interactions, particularly the $C^{\delta-}$–$C^{\delta-}$ nonbonded interactions (2.79 Å in the cubic phase, compared with 2.85 Å in the β phase).

The tetragonal and pseudocubic defect zinc-blende structures, as well as the hexagonal defect wurtzite structure, all have low P-C-P bond angles (111°–115°) and correspondingly high energies. The monoclinic and orthorhombic defect wurtzite structures are lower in energy because the bond lengths and angles are closer to the strain-free values; C–C bonds are present in the optimized structures.

When the positions of carbon and phosphorus atoms in the graphitic structures are swapped relative to those in P_4C_3, the valencies of the atoms are not satisfied (the carbon atoms are two coordinated and the phosphorus atoms are three coordinated, as shown in Fig. 5 but with the carbon and phosphorus positions interchanged), resulting in highly unstable structures. Indeed, these structures were found to be high in energy when the symmetry was constrained (Table IV), while removing the symmetry constraint led to dramatic reconstructions.

The P_3C_4 formula unit contains an odd number of valence electrons (31) and the band gaps of the optimized crystal structures reveal metallic behavior. If the formula unit is instead taken as P_6C_8, the phosphorus and carbon atoms have 30 and 32 valence electrons available for bonding, respectively, which implies that structures with insulating character can be produced if each P_6C_8 formula unit contains one C–C bond.

Indeed, the two low-energy highly disordered structures derived from the wurtzite structure include, in addition to P–C bonding, one C–C bond per P_6C_8 unit (see previous discussion), making these structures nonmetallic. Given that these structures are relatively low in energy, we further investigated the lowest-energy metallic structures (α-, β-, and cubic C_3N_4) with one C–C bond per P_6C_8 unit introduced by displacement of the carbon atoms in the initial structures. For this formally closed-shell structure, we have considered two possible scenarios for the α- and β-C_3N_4 structure geometries and four different reconstructions for the cubic-C_3N_4 case obtained by displacing different pairs of carbon atoms. The lowest-energy form obtained starting from each of the three structures is shown in Fig. 7, with the C–C bonds highlighted.

In all three cases, the structures with one C–C bond per P_6C_8 unit are lower in energy than the structures without carbon bonds (Fig. 8). The energy decreases associated with

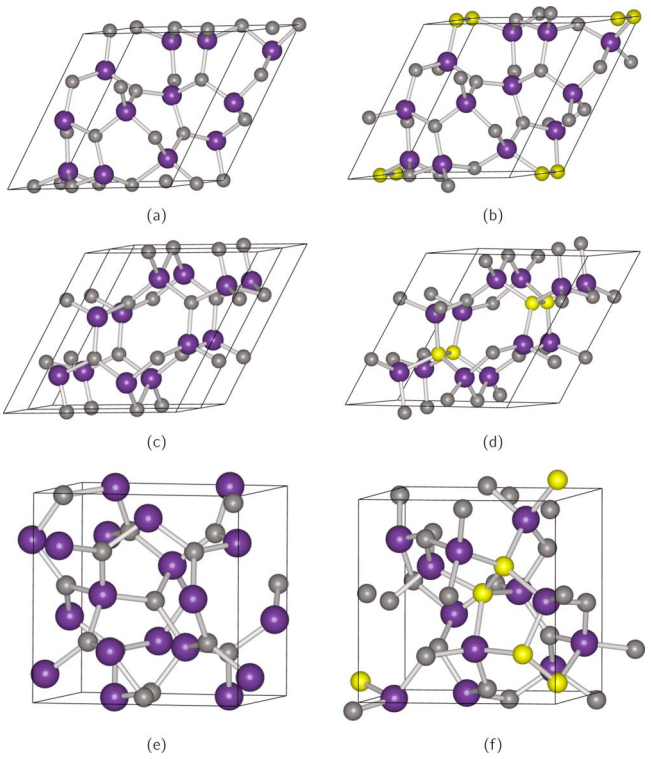

FIG. 7. (Color online) $P_{12}C_{16}$ unit cells for calculated structures structure: (a) and (b) are derived from the α-C_3N_4 structure, with and without one C–C bond per P_6C_8 unit, respectively, (c) and (d) are derived from the β-C_3N_4 structure with and without one C–C bond per P_6C_8 unit, respectively, and (e) and (f) are derived from the cubic-C_3N_4 structure, with and without one C–C bond per P_6C_8 unit, respectively. The light gray and the darker purple atoms are C and P, respectively, and the black lines show the unit-cell boundaries. Carbon atoms involved in the C–C bonds are shown in yellow.

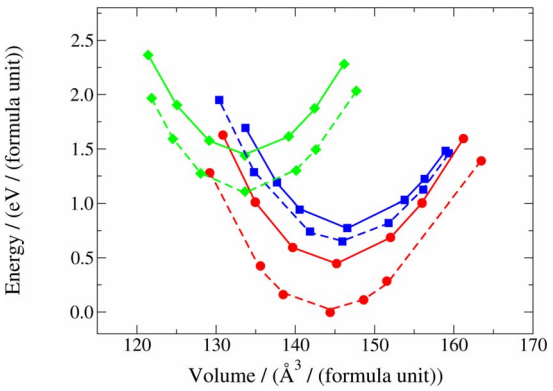

FIG. 8. (Color online) Energy per P_6C_8 formula unit as a function of volume for the three lowest-energy crystal structures for P_3C_4 shown in Fig. 7 [structures are derived from β-C_3N_4 (red circles), α-C_3N_4 (blue squares), and cubic C_3N_4 (green diamonds)]. Solid line: original structures without C–C bonds; dashed line: structures with 1 C–C bond per P_6C_8 unit. The lines show the fit of the data to the Birch-Murnaghan equation of state (Ref. 39). Energies are relative to the lowest-energy structure.

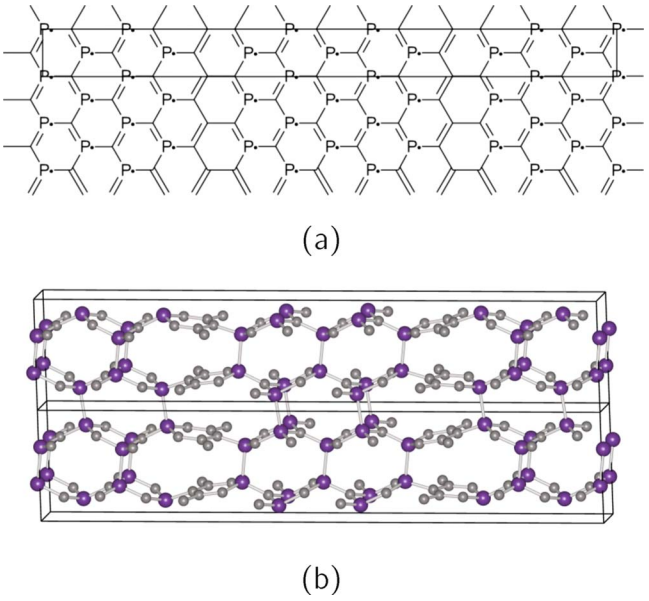

FIG. 9. (Color online) β-InS-like structure for P_3C_4. (a) Structural motif for a single layer and (b) optimized structure. The light gray and the darker purple atoms are C and P, respectively, and the black lines show the unit-cell boundaries.

introducing a C–C bond in the structure are 0.14, 0.45, and 0.37 eV per C_8P_6 formula unit for the α-, β-, and cubic-C_3N_4 structures, respectively. The α-C_3N_4-related structure with a C–C bond shows significant distortion from the ideal C sp^3-bonding environment and the P-C-P bond angle for sp^2 carbon ($\sim$117.0°) is even lower than in the structure without C–C bonds ($\sim$117.5°), indicating that the C–C bond introduces considerable strain. Structures derived from β- and cubic-C_3N_4 with C–C bonds are less strained and the energy decrease accompanying the introduction of the C–C bond is larger for both of these than for α-C_3N_4 (Fig. 8).

We have seen that the lowest-energy structure for both PC and PC_3 is a β-InS-like structure with sp^2 carbon, four-coordinate hypervalent phosphorus, and P–P bonding. This structure can be easily modified to a range of stoichiometries by changing the sp^2 carbon concentration. Therefore, it was thought that there may be a related structure that is low in energy for P_3C_4. This was indeed found to be so, and a β-InS-related structure (Fig. 9) is the lowest-energy structure we have found for P_3C_4 (Table IV). This is a relatively strain-free structure, with an average P-C-P bond angle of 119.9°, average C-P-C/C-P-P bond angle of 109.3°–109.4°, P-P interlayer bond lengths of 2.22–2.23 Å and intralayer C-P bond lengths of 1.70–1.72 Å, indicating double-bond character.

The bulk modulus, calculated from the energy versus volume curves (Fig. 8), is 236, 213, and 234 GPa for the α-, β-, and cubic-C_3N_4-like phases (for the low-energy structures that contain C–C bonds), respectively. These are the highest bulk moduli for any of the structures investigated in this work. The bulk modulus of the β-InS-like structure, the lowest-energy structure that we have found for P_3C_4, is 126 GPa.

Band structures have also been investigated briefly. As we have seen, structures without C–C bonds are metallic. When the valencies are satisfied by including one C–C bond per P_6C_8 formula unit for the α-, β-, and cubic-C_3N_4 structures, the energy is lower and insulating behavior is predicted. The band gap for the lowest-energy β-C_3N_4 structure is 2.0 eV with GGA and 3.0 eV with B3LYP. This indirect band gap is larger than that calculated for more phosphorus-rich stoichiometries, suggesting that increasing carbon content corresponds to an increased band gap. These results, together with the results for the β-InS-like structures of PC, also suggest that the presence of hypervalent phosphorus corresponds to a larger band gap relative to structures with three-coordinate phosphorus, although further data are required to confirm this trend.

D. Discussion: Properties of P_xC_y and general trends

1. Thermodynamic stability and cohesive energy

Formation energies have been calculated for the different stoichiometries from black phosphorus and graphite and are shown in Fig. 10(a). The structures are grouped into three families: graphitelike structures (sp^2 carbon and phosphorus) and pseudocubiclike structures (sp^3 carbon and phosphorus), produced as discussed in previous publications,[16,18] as well as β-InS-like structures (sp^3 hypervalent phosphorus and sp^2 carbon) with P–P interlayer bonds and varying amounts of three-coordinate carbon between the phosphorus atoms. Data from previous publications[11,18] are included for additional stoichiometries (PC_3, P_4C_{11}, P_4C_{19}, P_4C_{27}, and P_4C_{35}). The values for carbon (graphite) and phosphorus (black) used to calculate these formation energies were −156.17 and −180.82 eV per atom, respectively.

It was noted previously[18] that the pseudocubiclike structures become more stable than graphitelike structures at a phosphorus mole fraction of $\sim$0.4. However, with the inclusion here of the β-InS-related structures, it can be seen that these structures become more stable than the graphiticlike structures at a lower phosphorus mole fraction of $\sim$0.2. They are more stable than the pseudocubiclike structures for all compositions up to a phosphorus mole fraction of 0.5, above which construction of β-InS-like structures is not possible due to the inclusion of a large number of weak P–P bonds. There is a maximum in the formation energy of phosphorus carbide at a phosphorus atomic fraction of $\sim$0.3.

The energetic favorability of structures containing hypervalent phosphorus depends on the phosphorus content. For PC, structures with hypervalent four-coordinate phosphorus are approximately equal in energy to those with three-coordinate phosphorus. When the P:C ratio is greater than 1, the inclusion of hypervalent phosphorus will necessitate formation of a significant number of P–P bonds, making hypervalent phosphorus unfavorable in this case; thus, the lowest-energy structures at a phosphorus mole fraction $>$0.5 are pseudocubiclike structures with three-coordinate phosphorus. However, for a P:C ratio of less than 1, the presence of hypervalent phosphorus will be favorable. Thus, for a phosphorus mole fraction $<$0.5 (and $>$0.2), β-InS-like structures

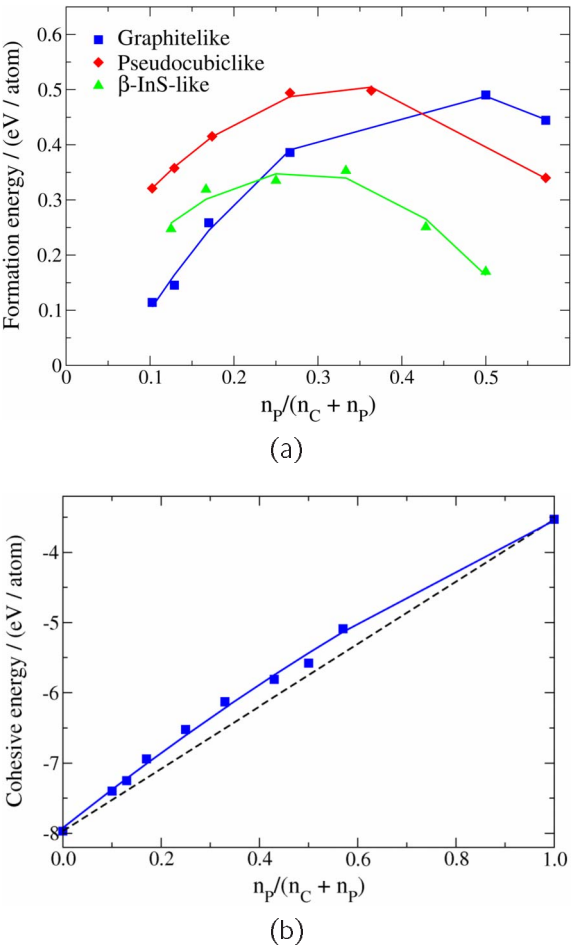

FIG. 10. (Color online) (a) Energy of formation as a function of phosphorus content for P_xC_y. The solid lines are parabolic fits to the data points and serve to guide the eye. (b) Cohesive energy for C (diamond), P (black P), and the most stable calculated P_xC_y structures; the dotted line connects the points for elemental C and P, while the solid line is a parabolic fit to the data points and serves to guide the eye.

with hypervalent phosphorus and sp^2, rather than sp^3, hybridized carbon are lowest in energy.

These results indicate that it is possible to group together structures with different compositions based on the local bonding of carbon and phosphorus and then analyze trends in the energies of these different groups of structures as a function of composition. This provides a systematic understanding of the preferred local environments of both carbon and phosphorus as a function of composition, from which it is possible to predict, for any composition, the preferred bonding environments for phosphorus and carbon and, hence, structures that are likely to be low in energy.

Figure 10(b) shows that the cohesive energies for all P_xC_y lie above the line connecting the values for pure P and pure C, indicating that all compositions are thermodynamically unstable with respect to the elements. Nevertheless, it may be possible to produce P_xC_y if the products are under kinetic control. In addition, significant density differences between the reactant elements and the products should be able to be exploited for the purposes of synthesis. For example, the volume of PC in the β-InS-like structure is 22.6 Å^3/f.u., compared with 9.23 Å^3 per atom for graphite (2.2 g/cm^3) (Ref. 48) and 20.6 Å^3 per atom for black phosphorus (2.69 g/cm^3).[48] We estimate ΔV for the formation of PC from graphite and black phosphorus to be ~5.6 Å^3/f.u. and thus that the formation of PC is thermodynamically favorable at an applied pressure of ~10 GPa (ignoring entropic contributions). The use of phosphorus as a catalyst for high-temperature/high-pressure transformation of graphite to diamond has been reported.[49,50] The diamond grown in this process was blue in color, attributed to the phosphorus contained in the diamond crystal. Our results indicate that high-pressure synthesis may well be a possible route to crystalline phosphorus carbide.

2. Bulk modulus

In general, the bulk modulus of phosphorus carbide increases as the ratio of the number of four-coordinated atoms to three-coordinated atoms increases, the carbon content increases, and also as C–C bonds are introduced. In the pseudocubic structure for P_4C_3, the carbon is four coordinated and the phosphorus is three coordinated, so the ratio of four-coordinate to three-coordinate atoms is 0.75. In the β-InS-like structure for PC, the ratio of four-coordinated to three-coordinated atoms is 1. In P_3C_4, in the α-, β-, and cubic-C_3N_4-like phases, all of the phosphorus and one carbon atom per P_3C_4 unit are four coordinated, so the ratio of four coordinated to three-coordinated atoms is 1.33. In accordance with these observations as well as the carbon content, these structures in order of increasing bulk modulus are $P_4C_3 < PC < P_3C_4$. However, there is no simple linear dependence between bulk modulus and the ratio of the number of four-coordinated to three-coordinated atoms, but it also depends on the local environment of carbon and phosphorus. For example, the bulk modulus of pseudocubic P_4C_3 is similar to that of PC in the β-InS-like structure with P–P interlayer bonds, despite having a lower ratio of four-coordinated to three-coordinated atoms and a lower carbon content. There is some double-bonding character in the PC structure, while there are only P–C single bonds in P_4C_3, and the carbon atoms are sp^2 rather than sp^3 hybridized, but there are also relatively weak P–P bonds. For PC, the bulk modulus increases as the P–P interlayer bonds are replaced with P–C bonds and increases further with C–C interlayer bonds; in all cases, the ratio of four-coordinated to three-coordinated atoms and the carbon content are the same. Finally, the bulk modulus of P_3C_4 in the α-, β-, and cubic-C_3N_4-like phases is approximately the same as that of PC with C–C interlayer bonds, despite having a higher ratio of four-coordinated to three-coordinated atoms and a higher carbon content; three out of four carbon atoms are sp^2 hybridized in the P_3C_4 structures (all carbon atoms are sp^3 hybridized in the PC structure with C–C interlayer bonds), but there are significantly fewer C–C bonds. The bulk modulus of the β-InS-related structure for P_3C_4 is low (only ~126 GPa), despite having a relatively high carbon content, consistent with the low ratio of four-coordinate to three-coordinate atoms (0.43). This structure also contains relatively weak P–P bonds. These results are in accordance with a similar asser-

tion of Mattesini and Matar[51] for the C_xN_y system that the bulk modulus of $C_{11}N_4$ is higher than C_3N_4, showing an increase in bulk modulus as the ratio of the number of four-coordinate atoms to three-coordinate atoms increases and as C–C bonds are introduced into the structure.

IV. CONCLUSIONS

Crystalline structures have been predicted for a range of phosphorus carbide stoichiometries. The trends in preferred local environments for phosphorus and carbon as a function of composition have been analyzed, making it possible to predict, for any composition, the most likely bonding environments that will be found in low-energy structures. When the phosphorus atomic fraction is >0.2, the structures with the lowest energies are always those that allow phosphorus to adopt a pyramidal geometry. When the phosphorus content is relatively high (e.g., P_4C_3), a combination of three-coordinate phosphorus and four-coordinate carbon is the most favorable arrangement, since this provides a structure that contains only C–P bonds. Thus, for P_4C_3, the lowest-energy structures are defect zinc blende, although the energy is relatively insensitive to the vacancy ordering. As the carbon content is increased, the lowest-energy structures are those that contain hypervalent four-coordinated phosphorus and sp^2 carbon, since with an increased carbon content this can be achieved without the necessity for the structure to contain a significant number of energetically unfavorable P–P bonds. Thus, for PC, PC_3, and P_3C_4, the lowest-energy structures are related to β-InS and contain sp^2 carbon and hypervalent four-coordinate phosphorus.

For all phosphorus carbide stoichiometries except P_3C_4, there is a set of related low-energy structures that are all close in energy. Attempts to synthesize phosphorus carbide are likely to result in production of a mixture of structures. All structures studied have positive formation energies with respect to the elements at ambient pressure, but these are predicted to decrease markedly at relatively modest pressures. The stoichiometries with the lowest formation energies are PC and very carbon-rich graphitic structures (with phosphorus atomic fractions <0.15).

The solid-state chemistry of P_xC_y is markedly different from the C_xN_y analogs. The low-energy structures for C_3N_4 (e.g., α- and β-C_3N_4) are high in energy for P_4C_3 because the planar geometry adopted by nitrogen in these structures is energetically unfavorable for phosphorus. Similarly, the pseudocubic structure, high in energy for C_3N_4, is the most stable for P_4C_3. Additionally, graphitic structures, lowest in energy for carbon nitride, have high energies for phosphorus carbide (except for structures that are very rich in carbon[18]) because a planar geometry and low coordination is unstable for phosphorus. Of the diamond-related structures, the structures lowest in energy for phosphorus carbide are often the same as the low-energy structures of carbon nitride, but with the positions of the carbon and group 15 element interchanged. This is the case for CN/PC, C_3N_4/P_3C_4, and C_3N/PC_3.

We have briefly examined the bulk modulus and band gaps of the lowest-energy structures. The bulk modulus generally increases as the ratio of the number of four-coordinated atoms to three-coordinated atoms increases, but it also depends on the local bonding environments. The band gap increases as the carbon content increases and is higher for structures with four-coordinate hypervalent phosphorus, relative to structures with three-coordinate phosphorus. These results suggest that at least some compositions and structures of phosphorus carbide may have useful electronic properties, such as wide-band-gap semiconductivity. We hope that our comprehensive study of P_xC_y structures will encourage and assist in the synthesis of these potentially useful materials.

ACKNOWLEDGMENTS

This work was supported by EPSRC Grant No. GR/N35328 and time on two supercomputer clusters (the Mott supercomputer cluster at RAL and the Dirac cluster at the University of Bristol) purchased and supported by JREI grants from HEFCE. J.N.H. acknowledges support from the Ramsay Memorial Fellowships Trust and J.M.O. acknowledges funding from the Spanish Ministry of Science and Innovation (project MAT2006-13646-C03-02). Helpful discussions with Paul May are gratefully acknowledged.

*Corresponding authors; judy.hart@bristol.ac.uk; n.l.allan@bristol.ac.uk

†Present address: Instituto de Química-Física "Rocasolano," CSIC, E-28006 Madrid, Spain.

[1] D. M. Teter and R. J. Hemley, Science **271**, 53 (1996).

[2] A. Crunteanu, R. Alexandrescu, S. Cojocaru, M. Charbonnier, M. Romand, and F. Vasiliu, J. Phys. IV **9**, Pr8-419 (1999).

[3] J. Wei, P. Hing, and Z. Q. Mo, Surf. Interface Anal. **28**, 208 (1999).

[4] D. X. Shi, X. F. Zhang, L. Yuan, Y. S. Gu, Y. P. Zhang, Z. J. Duan, X. R. Chang, Z. Z. Tian, and N. X. Chen, Appl. Surf. Sci. **148**, 50 (1999).

[5] X. Yan, T. Xu, G. Chen, S. Yang, H. Liu, and Q. Xue, J. Phys. D **37**, 907 (2004).

[6] I. Widlow and Y. W. Chung, Int. Mater. Rev. **47**, 153 (2002).

[7] E. Kroke and M. Schwarz, Coord. Chem. Rev. **248**, 493 (2004).

[8] L. Yang, P. W. May, L. Yin, Y. Huang, J. A. Smith, and T. B. Scott, Nanotechnology **18**, 335605 (2007).

[9] L. Yang, P. W. May, L. Yin, T. B. Scott, J. A. Smith, and K. N. Rosser, Nanotechnology **17**, 5798 (2006).

[10] S. R. J. Pearce, P. W. May, R. K. Wild, K. R. Hallam, and P. J. Heard, Diamond Relat. Mater. **11**, 1041 (2002).

[11] F. Claeyssens, G. M. Fuge, N. L. Allan, P. W. May, and M. N. R. Ashfold, Dalton Trans. **2004**, 3085.

[12] A. T. L. Lim, Y. P. Feng, and J. C. Zheng, Mater. Sci. Eng., B **99**, 527 (2003).

[13] J. C. Zheng, M. C. Payne, Y. P. Feng, and Adele Tzu-Lin Lim, Phys. Rev. B **67**, 153105 (2003).
[14] E. Kim, C. Chen, T. Kohler, M. Elstner, and T. Frauenheim, Phys. Rev. Lett. **86**, 652 (2001).
[15] M. Côté and M. L. Cohen, Phys. Rev. B **55**, 5684 (1997).
[16] M. Mattesini, S. F. Matar, and J. Etourneau, J. Mater. Chem. **10**, 709 (2000).
[17] F. Claeyssens, N. L. Allan, P. W. May, P. Ordejón, and J. M. Oliva, Chem. Commun. (Cambridge) **2002**, 2494.
[18] F. Claeyssens, J. M. Oliva, P. W. May, and N. L. Allan, Int. J. Quantum Chem. **95**, 546 (2003).
[19] S. J. Clark, M. D. Segall, C. J. Pickard, P. J. Hasnip, M. J. Probert, K. Refson, and M. C. Payne, Z. Kristallogr. **220**, 567 (2005).
[20] J. P. Perdew and Y. Wang, Phys. Rev. B **45**, 13244 (1992).
[21] J. M. Soler, E. Artacho, J. D. Gale, A. García, J. Junquera, P. Ordejón, and D. Sánchez-Portal, J. Phys.: Condens. Matter **14**, 2745 (2002).
[22] D. Vanderbilt, Phys. Rev. B **41**, 7892 (1990).
[23] P. Hohenberg and W. Kohn, Phys. Rev. **136**, B864 (1964).
[24] W. Kohn and L. J. Sham, Phys. Rev. **140**, A1133 (1965).
[25] N. Troullier and J. L. Martins, Phys. Rev. B **43**, 1993 (1991).
[26] L. Kleinman and D. M. Bylander, Phys. Rev. Lett. **48**, 1425 (1982).
[27] The pseudopotentials for carbon and phosphorus were generated with the following atomic configurations and cutoff radii for the *s*, *p*, and *f* components respectively: C→[He]$2s^2 2p^2$, 1.25 a.u. for all components and P→[Ne]$3s^2 3p^3$, 1.85 a.u. for all components.
[28] R. Dovesi, V. R. Saunders, C. Roetti, R. Orlando, C. M. Zicovich-Wilson, F. Pascale, B. Civalleri, K. Doll, N. M. Harrison, I. J. Bush, Ph. D'Arco, and M. Llunell, *CRYSTAL06 User's Manual* (University of Torino Press, Torino, 2006).
[29] R. Orlando, R. Dovesi, C. Roetti, and V. R. Saunders, J. Phys.: Condens. Matter **2**, 7769 (1990).
[30] A. Lichanot and M. Causà, J. Phys.: Condens. Matter **9**, 3139 (1997).
[31] A. D. Becke, J. Chem. Phys. **98**, 5648 (1993).
[32] C. Lee, W. Yang, and R. G. Parr, Phys. Rev. B **37**, 785 (1988).
[33] D. Pettifor, *Bonding and Structure of Molecules and Solids* (Oxford University Press, Oxford, 1995), Chap. 1.
[34] J. N Hart, F. Claeyssens, N. L. Allan, and P. W. May (unpublished).
[35] H. H. Karsch and E. Witt, J. Organomet. Chem. **529**, 151 (1997).
[36] R. O. Jones and O. Gunnarsson, Rev. Mod. Phys. **61**, 689 (1989).
[37] H. Goldwhite, *Introduction to Phosphorus Chemistry* (Cambridge University Press, Cambridge, 1981).
[38] N. N. Greenwood and A. Earnshaw, *Chemistry of the Elements*, 2nd ed. (Butterworth-Heinemann, Oxford, 1997).
[39] F. Birch, J. Geophys. Res. **83**, 1257 (1978).
[40] H. Yao, L. Ouyang, and W.-Y. Ching, J. Am. Ceram. Soc. **90**, 3194 (2007).
[41] C. Kittel, *Introduction to Solid State Physics*, 6th ed. (Wiley, New York, 1986).
[42] W. B. Pearson, *Crystal Chemistry and Physics of Metals and Alloys* (Wiley, New York, 1972).
[43] L. S. Bartell and L. O. Brockway, J. Chem. Phys. **32**, 512 (1960).
[44] I. Alves, G. Demazeau, B. Tanguy, and F. Weill, Solid State Commun. **109**, 697 (1999).
[45] D. P. Birnie III, W. C. Mackrodt, and W. D. Kingery, in *Nonstoichiometric Compounds: Advances in Ceramics*, edited by C. R. A. Catlow and W. C. Mackrodt (The American Ceramic Society, Westerville, OH, 1987), Vol. 23.
[46] F. Ding and Y. P. Feng, Comput. Mater. Sci. **30**, 364 (2004).
[47] R. M. Martin, *Electronic Structure: Basic Theory and Practical Methods* (Cambridge University Press, Cambridge, England, 2004).
[48] *CRC Handbook of Chemistry and Physics*, 88th ed., edited by D. R. Lide (CRC, Boca Raton, FL/Taylor and Francis, London, 2008).
[49] M. Akaishi, H. Kanda, and S. Yamaoka, Science **259**, 1592 (1993).
[50] Yu. Pal'yanov, I. Kupriyanov, A. Khokhryakov, Yu. Borzdov, V. Gusev, and J. Van Royen, Diamond Relat. Mater. **12**, 1510 (2003).
[51] M. Mattesini and S. F. Matar, Phys. Rev. B **65**, 075110 (2002).